Article

The Effects of Glaucoma Drainage Devices on Oxygen Tension, Glycolytic Metabolites, and Metabolomics Profile of Aqueous Humor in the Rabbit

Blake K. Williamson[1], Nathan M. Hawkey[1], Diane A. Blake[2], Joshua W. Frenkel[1], Kevin P. McDaniel[1], Justin K. Davis[3], Celine Satija[1], Alex Beazer[1], Suraj Dhungana[4,5], James Carlson[5,6], Susan McRitchie[5,7], and Ramesh S. Ayyala[1]

[1] Department of Ophthalmology, Tulane University School of Medicine, New Orleans, LA, USA
[2] Department of Biochemistry and Molecular Biology, Tulane University School of Medicine, New Orleans, LA, USA
[3] Center for Computational Science and Tulane University School of Public Health and Tropical Medicine, New Orleans, LA, USA
[4] Waters Corporation, Milford, MA, USA
[5] RTI International, Research Triangle Park, NC, USA at the time the work was performed
[6] LECO Corporation, St. Joseph, MI, USA
[7] University of North Carolina at Chapel Hill, Nutrition Research Institute, Eastern Regional Comprehensive Metabolomics Resource Core, Chapel Hill, NC, USA

Purpose: Glaucoma drainage device (GDD) implantation can lead to corneal decompensation. We evaluated changes over time in oxygen tension and in the metabolic environment of the aqueous humor after GDD implantation in the rabbit eye.

Methods: Ahmed Glaucoma Valves were implanted in the left eyes of eight male New Zealand white rabbits. Right eyes were used as a control. Oxygen tension was measured immediately before surgery and at 1 and 2 months postoperation. Aqueous humor was collected from the surgical and control eyes at 1, 2, and 5 months postoperation. Aqueous humor samples collected at 1 and 5 months postoperation were selected for broad-spectrum metabolomics analysis using ultra-performance liquid chromatography-time of flight-mass spectrometry (UPLC TOF-MS). Multivariate analysis methods were used to identify metabolite profiles that separated the surgical and control eye at 1 and 5 months.

Results: There was a significant decrease in oxygen tension in aqueous humor of the surgical eyes (9 mm Hg, 95% confidence interval [CI]: −14.7 to −3.5). Differences in the metabolic profiles between the surgical and control eye at 1 and 5 months were observed, as were differences for the surgical eye at 1 and 5 months. In addition, a metabolite profile was identified that differentiated the surgical eyes at 1 and 5 months.

Conclusion: Changes in the oxygen tension and metabolic intermediates occur within the aqueous humor as early as 1 month after GDD implantation.

Translational Relevance: Corneal decompensation following GDD implantation could be secondary to disruption of the normal aqueous circulation, resulting in hypoxia and an altered metabolic profile. Alterations to the GDD design might minimize aqueous disruption and prevent corneal decompensation.

Introduction

Glaucoma is a class of ocular diseases that lead to progressive optic nerve damage and retinal ganglion cell death, which results in distinctive patterns of impairment to the visual field.[1] Glaucoma affects over 70 million people and is the leading cause of irreversible blindness worldwide.[2–4] The primary goal of treatment is to slow disease progression by reducing intraocular pressure (IOP).[5] Prostaglandin analogues are commonly used as first-line medical therapy.[6] Surgery is indicated in patients whose IOP is not adequately controlled with conservative therapy and in those with severe disease.[6,7] A trabeculectomy is the most frequent surgical procedure performed to lower IOP. Glaucoma drainage devices (GDDs) are generally reserved for use after standard filtering surgery (trabeculectomy) has failed; however, an increasing number of ophthalmologists are recommending implantation of GDDs as the primary surgical intervention.[8] Recent studies have demonstrated that GDDs provide similar IOP reduction as trabeculectomy with superior 5-year success rates.[8–10] Furthermore, in favorable cases, GDDs have been shown to control IOP for more than 15 years postoperatively.[11]

The complications of GDDs can be divided into both short-term (within 5 years of surgery) and long-term (greater than 5 years after surgery). These include immediate hypotony, erosion of the tube, strabismus, infection, capsule fibrosis, and clinical failure. Furthermore, a common but poorly understood complication is an observed corneal endothelial cell loss over time leading to corneal decompensation.[8,12] Corneal decompensation is seen in up to 30% of patients who receive GDDs alone and in up to 51% of patients who have received a penetrating keratoplasty before, in combination with, or after GDD.[13–15] Known risk factors for reduced corneal endothelial cell density (ECD) include inflammation, peripheral anterior synechiae, and tube contact with uveal tissues or with the cornea.[15–17] The underlying mechanism for this commonly observed phenomenon has been elusive. Reduced ECD is observed frequently in cases where the tube is placed at a safe distance from the uveal and corneal tissues, which sheds doubt on the notion of mechanical trauma being the sole cause of endothelial cell loss.[18]

Various mechanisms have been proposed to explain the endothelial cell loss in patients with GDDs. McDermott and colleagues[18] have suggested that turbulence of aqueous humor present at the tip of the implant may be responsible for the observed reduction in ECD. This theory was further supported by a recent study that found reduced ECD was most prominent near tube placement. However, these findings were not statistically significant.[19] Furthermore, it is thought that GDDs can damage the corneal endothelium by permitting retrograde introduction of inflammatory cells into the anterior chamber.[15,17,20,21] In addition to retrograde flow of inflammatory cells, GDDs disrupt the blood-aqueous barrier, which was found to further increase influx of oxidative, apoptotic, and inflammatory mediators leading to endothelial cell damage.[22] Despite these findings, the precise etiology of reduced ECD and corneal decompensation following GDD placement has yet to be elucidated.

Aqueous humor is the biologic fluid that acts as a blood surrogate to supply nutrition to the avascular cornea and lens.[23] Proper aqueous humor dynamics is essential for the delivery of proper nutrients to the corneal endothelium and stroma. A temperature gradient in the anterior chamber creates a convective flow pattern due to a cooler temperature near the cornea and warmer temperature near the lens.[24] In cases where normal physiologic convective flow may be disrupted or altered, such as with GDDs, delivery of essential nourishment to the cornea may be disrupted and alterations to the metabolic microenvironment within the anterior chamber might be expected. Metabolomics uses analytical and mathematical methods to compare metabolites present within biological samples; it is a powerful tool that can provide detailed information about specific cellular processes.[25,26]

In this study, we investigated the oxygen tension, glycolytic metabolites, and the broad-spectrum metabolomics profile of rabbit aqueous humor after insertion of an Ahmed Valve GDD. The purpose behind our analysis was to explore the consequences of GDD implantation on the metabolic microenvironment of aqueous humor and how that may lead to corneal decompensation. These findings may lead to future therapeutic strategies that could improve long-term outcomes in patients who undergo implantation of GDDs for glaucoma.

Methods

Rabbits

Eight male New Zealand albino rabbits (Charles River, Wilmington, MA), weighing from 2.0 to 2.5 kg

(9–11 weeks old) were used for these studies. All studies adhered to the ARVO Statement for the Use of Animals in Ophthalmic and Vision Research and were approved by the Tulane University Institutional Animal Care and Use Committee (IACUC). Both eyes of each rabbit were involved in the study. The left eye served as the surgical eye and the right eye served as the control. All eyes were examined by slit-lamp and indirect ophthalmoscope prior to the study to exclude any pre-existing abnormalities. Upon arrival to Tulane University Health Sciences Center, the rabbits were given 7 days to acclimate to their environment. On day 8, bilateral aqueous humor oxygen measurements were performed. The right eye was measured first. The left eye was draped but the lid was left open/not taped shut during the procedure, which took 4 minutes or less. Aqueous humor samples were then collected and stored on ice until they could be aliquoted and frozen. Surgical implantation of an Ahmed valve was performed in the left eye of each rabbit as described below. The right eye served as a control. Additional bilateral aqueous humor oxygen measurements were performed at 27 days, and 52 days postoperatively. Bilateral aqueous humor samples were collected at 51 days postoperatively for analysis of glucose and lactate. Aqueous humor samples collected preoperatively and at 27 and 123 days postoperatively were used for broad-spectrum metabolomics analysis.

Anesthesia

Rabbits were anesthetized via intramuscular injection of a mixture that contained ketamine hydrochloride (20–35 mg/kg body weight) and xylazine (1–3 mg/kg body weight). Topical proparacaine eye drops (0.5%) were used to reduce discomfort.

Surgery

Animal surgeries for all experiments were performed as described below and in previous studies.[27–29] Sterile instruments were used and sterile surgical gloves and masks were worn. The animals were anesthetized as described above. The areas of the eyes were shaved and the eyelashes were trimmed to prevent hair from contaminating the field, and drapes were placed in a sterile fashion. The rabbit eye was then prepped with 5% betadine solution and subsequently covered with a sterile drape. Topical proparacaine eye drops (0.5%) were used to prevent further discomfort. A lid speculum was inserted to keep the lids apart. A 7-0 Vicryl suture was inserted

through the 12:00 PM limbus to inferiorly rotate the eye. Limbal peritomy was then performed in the superior temporal region. Dissection was carried posteriorly in the sub tenons' plane. The Ahmed glaucoma valve (Model FP-8) was primed with balanced salt solution, and the end plate was inserted into the sub tenons pocket and secured to the underlying sclera with interrupted 10–0 nylon sutures. The open end of the device's silicone tube was then inserted into the anterior chamber through a 23-guage butterfly needle tract. The conjunctiva was then secured to the limbus with interrupted 10–0 Vicryl sutures. A drop of cyclogyl 1% and tobradex ointment was instilled into the eye and then the lid speculum was removed from the eye.

Postoperative Care

Postoperatively, the rabbits received one dose of buprenorphine (0.03 mg/kg Im/SQ) and then as needed for pain. Animals were monitored until recovery from anesthesia. All rabbits were treated with topical Vigamox and Predforte QID for 7 days to prevent infection.

Aqueous Humor Acquisition

Aqueous humor was collected from both eyes before surgery, then at 27, 52, and 123 days postoperatively. Animals were anesthetized as previously described. After adequate anesthesia, the eye was prepped with 5% betadine solution and then covered with a sterile drape. A sterile 27G needle was inserted into the anterior chamber through the clear cornea of the para-limbal area. Approximately 0.1 mL aqueous humor was acquired in each collection cycle. The samples were immediately placed over an ice bath then transferred to a freezer for storage at $-70°C$.

In Vivo Oxygen Analysis

Oxygen content was measured using the OxyLite™ oxygen monitoring system with oxygen/temperature bare-fiber sensor manufactured by Oxford Optronix (Milton, UK). This company generously provided an 8-week loan of the OxyLite™ instrument for this study. The OxyLite™ system measures the partial pressure of oxygen (pO_2) in aqueous conditions by determining absolute dissolved oxygen. The oxygen sensing mechanism utilizes fluorescence quenching and fiber-optic technology.[30] The oxygen content of both eyes in each rabbit were measured at the time of surgery, and 27 and 53 days postoperatively. Animals

were anesthetized as previously described. After adequate anesthesia, the eye was prepped with 5% betadine solution and then covered with a sterile drape. The oxygen measurements were performed via a clear corneal incision in the para-limbal area with a 1-mm paracentesis blade to allow for exposure of anterior chamber in order to insert the oxygen detector probe. The oxygen/temperature bare-fiber probe was inserted through the incision until the tip of the probe was located in the center of the anterior chamber. The probe obtained measurements every 5 seconds and was held in the anterior chamber for 2 minutes, collecting a total of 24 measurements. A drop of cyclogyl 1% and tobradex ointment was then instilled into the eye. Postoperative care was performed as described above. Regression analysis of the oxygen tension in the surgical eye compared to the nonsurgical eye was performed.

Glucose and Lactate Analyses

Colorimetric analyses of glucose and lactate were performed on aqueous humor samples collected 53 days postoperatively. The same researcher performed all glucose and lactate measurements. The aqueous humor samples were defrosted and an aliquot of each was removed for analysis. The remaining volume of aqueous humor was returned to the freezer for storage at −70°C. Samples were analyzed in quadruplicate (sample dilution, 1:50) using either a Glucose Assay Kit (ab65333, Abcam, Cambridge, MA) or a Lactate Assay kit (MAK064, Sigma-Aldrich, St. Louis, MO). Both assays utilized the methods described by the manufacturers. The 96-well plates were read at 570 nm using a VersaMax Tunable Microplate reader from Molecular Biosystems. For glucose measurement, the coefficients of variation (CV = SD/mean) ranged from 1.9% to 10.9% in the 16 aqueous samples, with an average CV of 5.7%. For lactate measurement, the CVs ranged from 1.3% to 13.5%, and the average CV was 11.0%. Concentrations of glucose and lactate in the surgical eyes were compared to the control eyes by t-test with 95% confidence limits and linear regression analysis.

Broad-Spectrum Metabolomics Analysis

All analytical raw data files, and processed data files, have been uploaded to www.metabolmics workbench.org. The 27- and 153-day postoperative aqueous humor samples were prepared individually for analysis. The preoperative samples taken on the day of surgery had limited sample volume, so equal volumes of individual samples from the surgical eye were pooled and three aliquots were created. The samples from the control eye were pooled in an identical manner, and three aliquots were created. In addition, small, equal aliquots of each postoperative study sample was pooled to create quality control (QC) samples. All postoperative study samples, three preoperative surgical eye samples, and three preoperative control eye pooled samples were randomized for extraction and analysis. The QC samples were analyzed at fixed intervals across all the analytical runs. All study samples and QC samples were prepared using the same method. Cold methanol with tryptophan-d5 internal standard (400 µL) was added to 30 µL aqueous humor for protein precipitation. After centrifugation at 16,000 rcf, 350 µL supernatant was lyophilized overnight and reconstituted in 100 µL 95:5 water to methanol ratio for broad-spectrum metabolomics analysis.

Samples were analyzed on a SYNAPT G2-Si QTOF mass spectrometer coupled to an Acquity UPLC (Waters Corporation, Milford, MA). Prior to analyzing the study samples, the column and the system were equilibrated with 10 injections of QC samples. A 5-µL aliquot of aqueous humor extract from study samples and pooled samples was injected for mass spectrometric analysis. The compounds were separated on a Waters Acquity BEH HSS T3 column (2.1 × 100 mm, 1.8-µm particle size) operating at 50°C using a reversed-phase chromatographic separation. A gradient mobile phase consisting of water with 0.1% formic acid (A) and methanol with 0.1% formic acid (B) were used as previously described.[31,32] All MS data were collected over 50 to 1000 m/z in ESI positive ion mode. Leucine enkephalin was used as the lock mass, and a lock mass scan was collected every 45 seconds and averaged over three scans to perform correction for any mass drift over the course of the analytical run. Source and desolvation temperatures were set at 110°C and 450°C, respectively.

The raw mass spectrometric data were processed (alignment, normalization, and peak picking) using Progenesis QI (Waters Corporation). The normalized data were mean centered and scaled by dividing by the square root of the standard deviation, and multivariate analysis methods (principal component analysis [PCA] and orthogonal partial least squares discriminant analysis [OPLS-DA]) were used to reduce the dimensionality and to visualize the study groups (SIMCA 14.1, MKS Umetrics, Umea, Sweden).[33,34] The PCA scores plot of the ultra-performance liquid chromatography-time of flight-mass spectrometry

(UPLC-TOF-MS) positive ion data from the postoperative study samples were used to ensure that the QC samples clustered in the center of the study samples from which they were derived, which has become a standard method for assessing the quality of broad-spectrum metabolomics data. The surgical and control eyes were assessed separately using PCA to examine clustering and identification of outliers. Two of the day 153 control eye samples were identified as outliers in multivariate space and removed from further analyses. OPLS-DA, which is a supervised analysis method, was used to identify peaks important to differentiating the study groups. Loadings plots and variable influence on projection (VIP) plots were inspected, and peaks that had a VIP > 2 were determined to be important for differentiating the study groups. The VIP statistic summarizes the importance of the peak in differentiating the study groups.[34] All models used a sevenfold cross-validation to assess the predictive variation of the model (Q^2). Statistical analyses were conducted using SAS 9.4 (SAS Institute, Inc, Cary, NC).

Putative identification of the signals differentiating the study groups was made using a database search against RTI-RCMRC's in-house exact-mass-retention-time library of standards and the Human Metabolome Database (HMDB).

Results

Postoperative Condition

The rabbits were monitored every day for 7 days postoperatively. Both eyes were examined during follow-up. No evidence of endophthalmitis was noted in the surgical eyes. One rabbit expired at 4 weeks postoperation secondary to anesthesia complications.

In Vivo Oxygen Analysis

No significant differences in oxygen content were found in the surgical versus control eyes at the time of surgery or 27 days postoperatively ($P > 0.05$). Oxygen tension was significantly lower in the surgical eye (14.44 ± 2.3 mm Hg) compared to the control eye (22.18 ± 3.8 mm Hg) at 53 days postoperatively ($P < 0.0015$). Oxygen tension of aqueous humor in the rabbits at time of surgery, 1 month postoperatively, and 2 months postoperatively is shown in Table 1A. Regression analysis of the oxygen tension in the surgical eye compared to the nonsurgical eye is shown in Table 1B. At 53 days postoperation (L3), there is a significant difference between the surgical and non-surgical eye; the oxygen tension in the aqueous humor was estimated to be between 7.44 and 9.15 mm Hg lower in the eye with the GDD. Because the OxyLite™ instrument had to be returned to the manufacturer at the end of 2 months, no further oxygen analyses were available for this study.

Glucose and Lactate Analysis, 60 Days Postoperatively

The mean concentration of glucose in aqueous humor was slightly greater in the surgical eyes than that in the control eyes, but the differences were not significant (7.87 and 6.85 mM, respectively; $P = 0.1875$). Additionally, no statistically significant differences in aqueous humor lactate concentrations were noted in surgical versus and control eyes (7.79 and 8.40 mM, respectively; $P = 0.1354$). The concentrations determined during these experiments were within the ranges previously reported for similar samples.[35–38] Glucose and lactate measurements for individual rabbits are shown in Supplementary Figure S1, available in Supplementary Material.

Broad-Spectrum Metabolomics Analysis

Approximately 6000 features were detected in each sample. These features are from metabolites, fragments, adducts, and possible degradation products of unstable metabolites. PCA shows clear differentiation of the aqueous humor samples collected pre- and postsurgery for the surgical eye (Fig. 1B) but no differentiation of pre- and postsurgery control eye samples (Fig. 1A). Supervised multivariate analysis (OPLS-DA) shows strong differentiation of the aqueous humor samples collected from the surgical eyes on different days (Fig. 2A). Aqueous humor from the surgical and control eyes also differentiated at both 1 and 5 months postoperation (Figs. 2B, 2C). The metabolites that were important in differentiating the study groups based on VIP > 2 are shown in Tables 2 and 3. Table 2 shows the metabolites with lower relative abundance in the surgical eye, and Table 3 shows the metabolites with increased relative abundance in the surgical eye. Citric acid and 3-hydroxydodecanedioic acid were important to differentiating the aqueous humor of the surgical and the control eyes and were decreased in the experimental eye at both 1 month and 5 months postoperation. In addition, 1-tetradecanoyl-glycerol differentiated the eyes at 1 month postoperation, and at 5 months postoperation glucose, tyrosine, and tyramine, and uric acid were important to differentiating the

Table 1A. Oxygen Tension of the Aqueous Humor Before Surgery and at 1 and 2 Months Postoperation

Rabbit ID	Eye	Day 0 Postoperation O$_2$ (mm Hg)[a]	Day 27 Postoperation O$_2$ (mm Hg)	Day 53 Postoperation O$_2$ (mm Hg)
1	Surgical	13.57 ± 0.074	15.40 ± 1.41	19.10 ± 3.55
1	Control	34.90 ± 3.03	15.17 ± 2.65	40.19 ± 13.64
2	Surgical	17.27 ± 0.85	23.69 ± 2.54	21.36 ± 2.33
2	Control	15.43 ± 1.51	24.30 ± 1.34	25.58 ± 2.33
3	Surgical	20.40 ± 1.45	10.07 ± 4.16	6.80 ± 1.69
3	Control	28.20 ± 0.10	16.21 ± 2.19	18.93 ± 1.78
4	Surgical	25.77 ± 2.32	19.77 ± 1.32	15.16 ± 2.10
4	Control	12.20 ± 1.10	13.63 ± 1.14	15.82 ± 2.22
5	Surgical	25.97 ± 2.40	17.07 ± 1.25	8.81 ± 0.70
5	Control	27.50 ± 0.44	23.72 ± 1.09	15.4 ± 2.67
6	Surgical	18.13 ± 1.03	13.75 ± 1.23	[b]
6	Control	27.80 ± 2.01	25.60 ± 1.50	[b]
7	Surgical	17.20 ± 0.20	15.49 ± 2.79	14.07 ± 2.89
7	Control	17.70 ± 0.46	17.34 ± 2.66	23.36 ± 3.46
8	Surgical	25.43 ± 1.50	14.52 ± 2.90	15.78 ± 2.33
8	Control	37.63 ± 0.45	23.06 ± 2.57	15.97 ± 3.26

[a] Reported as mean ± SD of 24 measurements taken over a 2-minute time period.
[b] Rabbit 6 was deceased prior to day 53 postoperation measurements.

experimental and control eyes. Four of these metabolites (3-hydroxydodecanedioic acid, citric acid, glucose, and tyrosine) as well as arginine were important to differentiating the surgical eye at 1 and 5 months postoperation and were decreased in the 5-month sample (Table 2). 1-Tetradecanoyl-glycerol and polysorbate 60 were increased in the surgical eye and important to differentiating the surgical and control eyes at 5 months postoperation. At 1 month postoperation, geranyl pyrophosphate and polysorbate 60 were important to differentiating the eyes and increased in the experimental group. 1-Tetradecanoyl-glycerol, polysorbate 60, and beta-aspartyl-glutamic acid were increased in the surgical eye at 5 months postoperation compared to 1 month and important to differentiating the eyes (Table 3). Additional information on a subset of metabolites responsible for differentiating the study groups is presented in the Supplementary Material.

Discussion

In this study, we investigated metabolic changes that occur to the aqueous humor after GDD implantation in the rabbit. Aqueous humor functions as a blood surrogate to deliver nutrition to the avascular tissues of the anterior chamber. Proper function of aqueous humor depends on convective flow, and GDD implantation may alter proper fluid dynamics. In order to develop a better understanding

Table 1B. Statistical Analysis of Oxygen Tension in the Surgical Versus Control Eyes[a]

Analysis of Maximum Likelihood Parameter Estimates

Parameter	Estimate	Standard Error	Wald 95% Confidence Limits		Wald χ^2	Pr > χ^2
L1	−1.2375	2.7104	−6.5497	4.0748	0.21	0.6480
L2	−3.5029	2.7104	−8.8151	1.8094	1.68	0.1962
L3	−9.153	2.8631	−14.7646	−3.5415	10.22	0.0014

[a] L1, 2, and 3 represent the estimated differences between surgical and nonsurgical eyes at time points before surgery, 27 days, and 53 days postoperation, respectively. L1 and L2 do not differ significantly from 0. At 53 days postoperation (L3), there is a significant difference between the surgical and nonsurgical eye, estimated to be 9.153 mm Hg lower in the eye with the GDD.
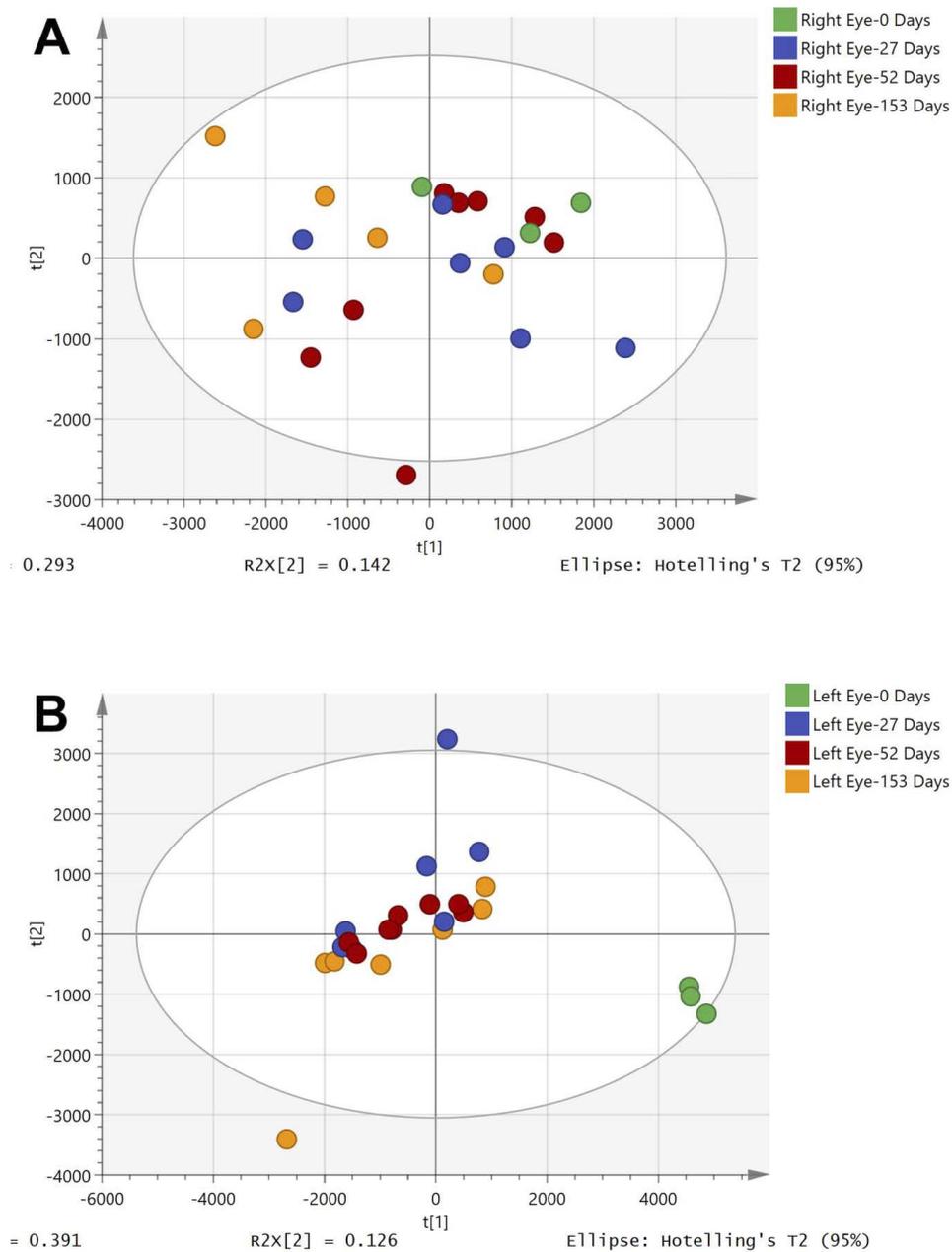
Figure 1. PCA of UPLC-TOF-MS positive ion metabolomics data for the aqueous humor samples. (A) Control eye (right eye) for preoperative pooled samples (control, *green circles*), day 27 (*blue circles*), day 52 (*red circles*), and day 153 (*orange circles*) excluding two outliers. (B) Surgical eye (left eye) for preoperative pooled samples (control, *green circles*), day 27 (*blue circles*), day 52 (*red circles*), and day 153 (*orange circles*).

of changes to the anterior chamber that occur after implantation of a GDD, we evaluated the oxygen tension, glycolytic metabolites, and the broad-spectrum metabolomics profile of aqueous humor.

A significant decrease in oxygen tension was found in the surgical eye at 2 months postoperation (Table 1B). Aerobic glycolysis is the principal pathway of metabolism in the human eye outside

of the lens.[39] Oxygen to the anterior chamber of the eye is primarily supplied by the atmosphere, limbal circulation, palpebral conjunctiva, and blood supply to the ciliary body and iris.[40] A recent study has demonstrated that oxygen tension in the aqueous humor is dependent on oxygen delivery by systemic circulation.[39] Our findings of decreased oxygen tension in the aqueous humor at 2 months post-
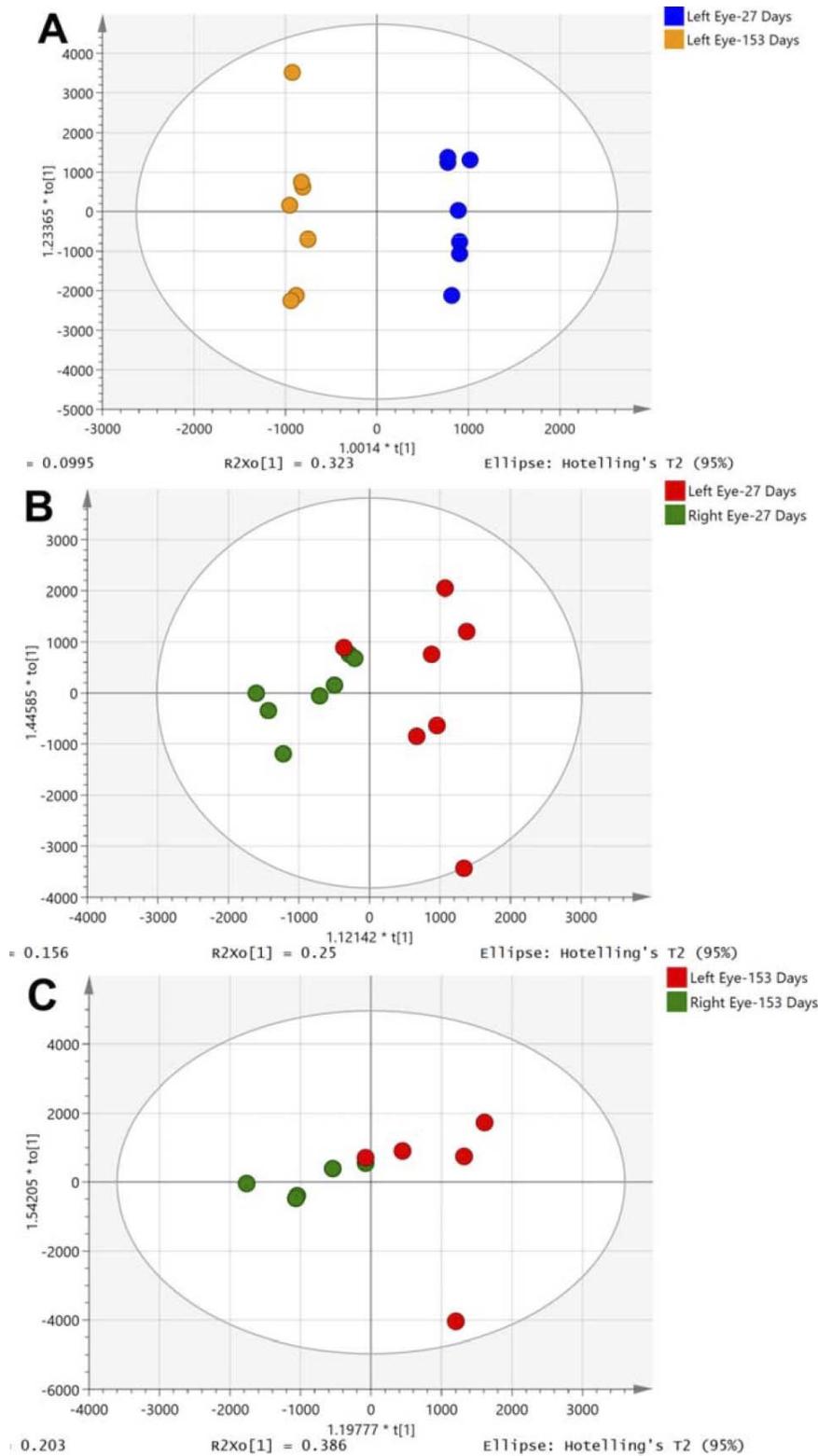
Figure 2. Supervised multivariate analysis (OPLS-DA) was used to visualize the separation of the phenotypic groups and to determine markers that differentiate the phenotypic groups. (A) Surgical eye: day 153 (*orange circles*) vs. day 27 (*blue circles*) (R2X = 0.65, R2Y = 0.99, Q2 = 0.62); (B) day 27: surgical eye (*red circles*) vs. control eye (*green circles*) (R2X = 0.41, R2Y = 0.72, Q2 = −0.30); (C) day 153: surgical eye (*red circles*) vs. control eye (*green circles*) excluding paired outliers (R2X = 0.59, R2Y = 0.70, Q2 = −0.79).

Table 2. Metabolites (VIP > 2) Important to Differentiating the Study Groups That Were Decreased in Either the Surgical Eye (Left) or Day 153 Surgical Eye

Surgical Eye: Day 153 vs. Day 27 ($n = 14$)

Metabolite	VIP	Fold Change (Surgical Eye Day 153/Day 27)	P-value[a]
Citric acid	3.7	0.8	0.18
3-Hydroxydodecanedioic acid	3.0	0.8	0.48
Glucose	2.8	0.9	0.37
Tyrosine	2.5	0.9	0.23
Arginine	2.1	0.8	0.02
Unknown compound (402.1827 m/z)	36.6	0.001	0.11
Unknown compound (239.0708 Dalton [Da])	8.3	0.3	0.01
Unknown compound (416.1991 m/z)	7.0	0.005	0.15
Unknown compound (402.3489 m/z)	6.5	Absent in day 153	0.19
Unknown compound (386.1736 Da)	6.5	0.1	0.19
Unknown compound (212.1169 m/z)	5.7	0.1	0.17
Unknown compound (358.1899 m/z)	5.7	0.02	0.12
Unknown compound (241.0684 Da)	4.8	0.4	0.01
Unknown compound (803.3593 m/z)	3.6	0.0004	0.25
Unknown compound (194.0487 Da)	3.2	0.3	0.01
Unknown compound (402.3984 m/z)	3.2	Absent in day 153	0.23
Unknown compound (204.0334 Da)	2.7	0.4	0.02
Unknown compound (215.0601 m/z)	2.5	0.2	0.13
Unknown compound (159.0841 Da)	2.4	0.3	<0.0001
Unknown compound (383.1801 m/z)	2.3	0.1	0.16
Unknown compound (415.1033 Da)	2.3	0.2	0.04
Unknown compound (262.0599 m/z)	2.3	0.4	0.01
Unknown compound (262.0600 m/z)	2.2	0.4	0.01
Unknown compound (255.0703 Da)	2.2	0.3	0.02

Surgical Eye vs. Control Eye: Day 27 ($n = 14$)

Metabolite	VIP	Fold Change (Surgical Eye Day 27/Control Eye Day 27)	P-value[a]
1-Tetradecanoyl-glycerol	17.3	0.8	0.57
3-Hydroxydodecanedioic acid	3.0	0.8	0.25
Citric acid	2.5	0.8	0.27
Unknown compound (824.8766 Da)	4.0	0.04	0.37
Unknown compound (239.0708 Da)	3.9	0.8	0.01
Unknown compound (344.2126 Da)	3.4	0.9	0.04
Unknown compound (825.3789 Da)	3.3	0.04	0.37
Unknown compound (241.0684 Da)	2.2	0.8	0.01

Surgical Eye vs. Control Eye: Day 153 ($n = 10$)

Metabolite	VIP	Fold Change (Surgical Eye Day 153/Control Eye Day 153)	P-value[a]
Glucose	5.2	0.9	0.12
Tyramine	4.5	0.9	0.27
Citric acid	4.1	0.8	0.29
Tyrosine	3.2	0.9	0.34

Table 2. Continued

Surgical Eye vs. Control Eye: Day 153 ($n = 10$)

Metabolite	VIP	Fold Change (Surgical Eye Day 153/Day 27)	P-value[a]
Uric acid	2.8	0.8	0.25
3-Hydroxydodecanedioic acid	2.1	0.6	0.18
Unknown compound (149.0773 Da)	12.3	0.9	0.03
Unknown compound (398.1704 Da)	6.6	0.1	0.24
Unknown compound (386.1736 Da)	3.9	0.3	0.38
Unknown compound (530.3101 m/z)	3.1	0.04	0.18
Unknown compound (486.3216 m/z)	3.0	0.02	0.23
Unknown compound (239.0708 Da)	2.5	0.7	0.02
Unknown compound (191.1509 Da)	2.2	0.1	0.20
Unknown compound (222.0698 Da)	2.1	0.8	0.002

Unknowns reported are those with VIP > 2 and either fold change < 0.5 or P-value < 0.05.

[a] Paired t-test.

operation suggest either decreased diffusion of oxygen into the aqueous from systemic circulation, which is unlikely, or increased consumption of oxygen due to an unidentified process, such as inflammation. Siegfried et al.[41] have suggested that the oxidative metabolism required to produce the ATP needed to secrete aqueous humor from the ciliary epithelial cells may be responsible for the low oxygen content observed near ciliary epithelium in rabbits, monkeys, and humans.[41,42] The other explanation could be a disturbance of convention currents. A temperature gradient in the anterior chamber creates a convective flow pattern due to a cooler temperature near the cornea and warmer temperature near the lens.[24] The oxygen-rich aqueous closer to the corneal endothelium would then migrate to the iris surface and gets sucked into the tube. This results in a disturbance of the convection currents that normally occur in the anterior chamber and dilution of oxygen-rich aqueous humor with aqueous with low oxygen content from the ciliary epithelium. Thus, disturbance in convection currents might also explain the aqueous hypoxia that was measured in these experiments. Hypoxia can certainly lead to corneal endothelial dysfunction and corneal edema as was evident from the hard contact lens experiments.[43]

Independent measures of glucose and lactate performed at 2 months postoperatively showed no significant differences (Supplementary Fig. S1). The relative peak intensity of glucose acquired through UPLC-MS broad-spectrum metabolomics had a 0.9-fold change in the surgical eye compared to the control eye at 153 days (Table 2), and this value was also nonsignificant; however, glucose was determined to be important to differentiating the surgical and control eyes based on the multivariate analysis, thus demonstrating the power of metabolomic versus single analyte investigations. The decrease in glucose concentration found in the surgical eye in our study may indicate increased consumption of glucose by inflammatory cells, other cells in the anterior chamber, or a physiologic variance. In a previous study using ^{1}H NMR broad-spectrum metabolomics comparing rat aqueous humor in control eyes and eyes with increased IOP/glaucoma induced by intracamerular injection of hyaluronic acid, glucose was found to be important to differentiating the eyes. The relative intensity of glucose was decreased in the glaucomatous eye.[44] In our study, glucose was also an important differentiator of the surgical and control eyes at 5 months postoperation as well as a differentiator of the experimental eye at 5 months compared to 1 month, and glucose was decreased in the experimental eye at 5 months compared to both the control eye at 5 months and the surgical eye at 1 month postoperation.

In the same rat study,[44] citrate, lipids/cholesterol, fatty acids, and glutamate + glutamine were found in the aqueous humor of the glaucomatous eye and were identified as being important to differentiating the eyes. Our study found similar differentiating metabolites (citric acid, 1-tetradecanoyl-glycerol, beta-aspartyl-glutamic acid, and 3-hydroxydodecanedioic acid).

Table 3. Metabolites (VIP > 2) Important to Differentiating the Study Groups That Were Increased in Either the Surgical Eye (Left) or Day 153 Surgical Eye

Surgical Eye: Day 153 vs. Day 27 (*n* = 14)

Metabolite	VIP	Fold Change (Surgical Eye Day 153/Day 27)	*P*-value[a]
1-Tetradecanoyl-glycerol	12.6	1.1	0.80
Polysorbate 60	3.3	1.1	0.28
Beta-aspartyl-glutamic acid	2.1	1.1	0.21
Unknown compound (375.2514 Dalton [Da])	20.5	10.4	0.001
Unknown compound (456.2481 Da)	5.7	67.2	0.34
Unknown compound (398.1704 Da)	4.5	3.5	0.39
Unknown compound (773.4948 m/z)	4.0	209.6	0.003
Unknown compound (317.1825 m/z)	3.5	47.4	0.29
Unknown compound (252.0926 Da)	3.1	3.1	0.01
Unknown compound (486.3216 m/z)	3.1	39.6	0.36
Unknown compound (421.3158 m/z)	2.9	6.4	0.001
Unknown compound (530.3101 m/z)	2.6	15.2	0.36
Unknown compound (231.0828 m/z)	2.4	2.6	0.02
Unknown compound (221.2324 m/z)	2.2	5.2	0.03
Unknown compound (276.0931 Da)	2.2	2.3	0.14

Surgical Eye vs. Control Eye: Day 27 (*n* = 14)

Metabolite	VIP	Fold Change (Surgical Eye Day 27/Control Eye Day 27)	*P*-value[a]
Geranyl pyrophosphate	2.1	7.5	0.30
Polysorbate 60	2.1	1.0	0.63
Unknown compound (402.1827 m/z)	44.2	514.3	0.11
Unknown compound (416.1991 m/z)	8.7	159.4	0.15
Unknown compound (402.3489 m/z)	8.3	Absent in control eye	0.19
Unknown compound (358.1899 m/z)	6.9	42.0	0.13
Unknown compound (803.3593 m/z)	4.8	1795.8	0.25
Unknown compound (212.1169 m/z)	4.4	10.6	0.18
Unknown compound (402.3984 m/z)	4.2	Absent in control eye	0.23
Unknown compound (215.0601 m/z)	3.1	4.7	0.12
Unknown compound (383.1801 m/z)	2.9	14.3	0.16
Unknown compound (219.0574 m/z)	2.2	46.2	0.11

Surgical Eye vs. Control Eye: Day 153 (*n* = 10)

Metabolite	VIP	Fold Change (Surgical Eye Day 153/Control Eye Day 153)	*P*-value[a]
1-Tetradecanoyl-glycerol	13.8	1.0	0.97
Polysorbate 60	3.9	1.1	0.33
Unknown compound (342.2841 Da)	2.6	1.2	0.04

Unknowns reported are those with VIP > 2 and either fold change > 2 or *P*-value < 0.05.
[a] Paired *t*-test.

In the current study, glucose, citric acid, 3-hydroxydodecanedioic acid, arginine, and tyrosine were identified as being important for differentiating the surgical eyes at 1 month and 5 months post-operation and were decreased in the eye with the implanted GDD at 5 months. 1-tetradecanoyl-glycerol, polysorbate 60, and beta-aspartyl-glutamic acid were increased at 5 months compared to 1 month post-

translational vision science & technology

operation. These findings are consistent with the expectation that the GDD would lower IOP; however, IOPs were not measured in the current study because it is very difficult to accurately measure rabbit IOPs with standard tonometry.[45]

A more complete discussion of selected metabolites identified in aqueous humor important to differentiating the study groups (glucose, citrate, arginine, 1-tetradecanoyl-glycerol, acyl-carnitine/carnitine, dicarboxylic fatty acids, and polysorbate) can be found in the Supplementary Material.

Limitations

The major limitation to this study was the duration of follow-up. Oxygen measurements were taken only during the first 2 months of follow-up because we had to return the OxyLite™ instrument to the manufacturer. We evaluated the metabolomics profiles for only 5 months after surgery. Corneal endothelial decompensation is a long-term complication after GDD implantation. This 5-month study may not have been enough time to detect important metabolic changes that occur in the aqueous chamber up to several years postoperatively. Future studies should follow subjects from initial GDD implantation until there is evidence of loss in corneal ECD.

Furthermore, there was not enough volume of aqueous humor collected at the time of implantation to individually analyze each sample in the broad-spectrum metabolomics analysis. Therefore, these preoperative control samples were pooled for the metabolomics analysis. Future studies should ensure adequate aqueous humor collection to better understand the variability in the control group.

Conclusion

While other investigators have used a metabolomics approach to study the effects of induced glaucoma in aqueous humor,[44] the present study, to our knowledge, provides the first where the measurements of oxygen tension and metabolomics analysis of aqueous humor have been combined to gain new insights into the effects of GDD implantation on corneal decompensation. This study has allowed us to generate metabolic profile plots that differentiate those eyes with implanted GDDs from control eyes. Further studies are in progress to elucidate the metabolic alterations that occur in the surgical eyes, with the ultimate goal of decreasing the corneal decompensation that can occur after long-term GDD implantation.

Acknowledgments

Disclosure: **B.K. Williamson,** None; **N.M. Hawkey,** None; **D.A. Blake,** None; **J.W. Frenkel,** None; **K.P. McDaniel,** None; **J.K. Davis,** None; **C. Satija,** None; **A. Beazer,** None; **S. Dhungana,** None; **J. Carlson,** None; **S. McRitchie,** None; **R.S. Ayyala,** None

References

1. Weinreb RN, Aung T, Medeiros FA. The pathophysiology and treatment of glaucoma: a review. *JAMA*. 2014;311:1901–1911.
2. Kingman S. Glaucoma is second leading cause of blindness globally. *Bull World Health Organ*. 2004;82:887–888.
3. Sbeity Z, Ritch R. Annual World Glaucoma Day. Enhancing awareness of glaucoma: a leading cause of preventable blindness. *J Med Liban*. 2010;58:120–121.
4. Quigley HA, Broman AT. The number of people with glaucoma worldwide in 2010 and 2020. *Br J Ophthalmol*. 2006;90:262–267.
5. Boland MV, Ervin AM, Friedman DS, et al. Comparative effectiveness of treatments for open-angle glaucoma: a systematic review for the U.S. Preventive Services Task Force. *Ann Intern Med*. 2013;158:271–279.
6. Kulkarni SV, Damji KF, Buys YM. Medical management of primary open-angle glaucoma: best practices associated with enhanced patient compliance and persistency. *Patient Prefer Adherence*. 2008;2:303–314.
7. Present M K. and new treatment strategies in the management of glaucoma. *Open Ophthalmol J*. 2015;9:89–100.
8. Minckler DS, Francis BA, Hodapp EA, et al. Aqueous shunts in glaucoma: a report by the

translational vision science & technology

American Academy of Ophthalmology. *Ophthalmology*. 2008;115:1089–1098.

9. Gedde SJ, Schiffman JC, Feuer WJ, Herndon LW, Brandt JD, Budenz DL. Treatment outcomes in the Tube Versus Trabeculectomy (TVT) study after five years of follow-up. *Am J Ophthalmol*. 2012;153:789–803.e782.

10. Minckler DS, Vedula SS, Li TJ, Mathew MC, Ayyala RS, Francis BA. Aqueous shunts for glaucoma. *Cochrane Database Syst Rev*. 2006; Cd004918.

11. Ah-Chan JJ, Molteno AC, Bevin TH, Herbison P. Otago Glaucoma Surgery Outcome Study: follow-up of young patients who underwent Molteno implant surgery. *Ophthalmology*. 2005; 112:2137–2142.

12. Barton K, Heuer DK. Modern aqueous shunt implantation: future challenges. *Prog Brain Res*. 2008;173:263–276.

13. Al-Torbak A. Graft survival and glaucoma outcome after simultaneous penetrating keratoplasty and ahmed glaucoma valve implant. *Cornea*. 2003;22:194–197.

14. Hong CH, Arosemena A, Zurakowski D, Ayyala RS. Glaucoma drainage devices: a systematic literature review and current controversies. *Surv Ophthalmol*. 2005;50:48–60.

15. Topouzis F, Coleman AL, Choplin N, et al. Follow-up of the original cohort with the Ahmed glaucoma valve implant. *Am J Ophthalmol*. 1999; 128:198–204.

16. Hau S, Scott A, Bunce C, Barton K. Corneal endothelial morphology in eyes implanted with anterior chamber aqueous shunts. *Cornea*. 2011; 30:50–55.

17. Kim CS, Yim JH, Lee EK, Lee NH. Changes in corneal endothelial cell density and morphology after Ahmed glaucoma valve implantation during the first year of follow up. *Clin Exp Ophthalmol*. 2008;36:142–147.

18. McDermott ML, Swendris RP, Shin DH, Juzych MS, Cowden JW. Corneal endothelial cell counts after Molteno implantation. *Am J Ophthalmol*. 1993;115:93–96.

19. Koo EB, Hou J, Han Y, Keenan JD, Stamper RL, Jeng BH. Effect of glaucoma tube shunt parameters on cornea endothelial cells in patients with Ahmed valve implants. *Cornea*. 2015;34:37–41.

20. Kirkness CM. Penetrating keratoplasty, glaucoma and silicone drainage tubing. *Dev Ophthalmol*. 1987;14:161–165.

21. McDonnell PJ, Robin JB, Schanzlin DJ, et al. Molteno implant for control of glaucoma in eyes after penetrating keratoplasty. *Ophthalmology*. 1988;95:364–369.

22. Anshu A, Price MO, Richardson MR, et al. Alterations in the aqueous humor proteome in patients with a glaucoma shunt device. *Mol Vis*. 2011;17:1891–1900.

23. Goel M, Picciani RG, Lee RK, Bhattacharya SK. Aqueous humor dynamics: a review. *Open Ophthalmol J*. 2010;4:52–59.

24. Heys JJ, Barocas VH. A boussinesq model of natural convection in the human eye and the formation of Krukenberg's spindle. *Ann Biomed Eng*. 2002;30:392–401.

25. Frederich M, Pirotte B, Fillet M, de Tullio P. Metabolomics as a challenging approach for medicinal chemistry and personalized medicine. *J Med Chem*. 2016;59:8649–8666.

26. Sumner S, Pathmasiri W, Carlson J, McRitchie S, Fennel T. Metabolomics. In: Hodgson RCSaE, ed. *Molecular and Biochemical Toxicology*. New York: J Wiley and Sons; 2016.

27. Ayyala R, Michelini-Norris B, Flores A, Haller E, Margo C. Comparison of different biomaterials for glaucoma drainage devices: part 2. *Arch Ophthalmol*. 2000;118:1081–1084.

28. Ayyala R, Zurakowski D, Monshizadeh R, et al. Comparison of double-plate Molteno and Ahmed glaucoma valve in patients with advanced uncontrolled glaucoma. *Ophthalmic Surg Lasers*. 2002; 33:94–101.

29. Sahiner N, Kravitz D, Qadir R, et al. Creation of a drug-coated glaucoma drainage device using polymer technology: In vitro and in vivo studies. *Arch Ophthalmol*. 2009;127:448–453.

30. OxyLite In vivo and in vitro oxygen monitoring. In: http://www.oxford-optronix.com/product20/page501/menu2/Tissue_Vitality_Monitoring/Oxygen_Monitors/OxyLite_.html#tab7-tab; 2013.

31. Dunn WB, Broadhurst D, Begley P, et al. Procedures for large-scale metabolic profiling of serum and plasma using gas chromatography and liquid chromatography coupled to mass spectrometry. *Nat Protoc*. 2011;6:1060–1083.

32. Dhungana S CJ, Pathmasiri W, McRitchie S, Davis M, Sumner S, Appt SE. Impact of a western diet on the ovarian and serum metabolome. *Maturitas*. 2016;92:134–142.

33. Trygg J, Holmes E, Lundstedt T. Chemometrics in metabonomics. *J Proteome Res*. 2007;6:469–479.

34. Eriksson L, Byrne T, Johansson E, Trygg J, Vikström C. *Multi- and Megavariate Data Analysis: Basic Principles and Applications*. 3rd ed. Umeå, Sweden: Umetric Academy; 2013.

translational vision science & technology

35. Bergmanson JP, Johnsson J, Soderberg PG, Philipson BT. Lactate levels in the rabbit cornea and aqueous humor subsequent to non-gas permeable contact lens wear. *Cornea*. 1985;4: 173–176.

36. Gaasterland DE, Pederson JE, MacLellan HM, Reddy VN. Rhesus monkey aqueous humor composition and a primate ocular perfusate. *Invest Ophthalmol Vis Sci*. 1979;18:1139–1150.

37. Riley MV. Intraocular dynamics of lactic acid in the rabbit. *Invest Ophthalmol*. 1972;11:600–607.

38. Chou C, Han C-Y, Kuo WC, Huang YC, Feng CM, Shyu JC. Noninvasive glucose monitoring in vivo with an optical heterodyne polarimeter. *Applied Opt*. 1998;37:3553–3557.

39. Sharifipour F, Idani E, Zamani M, Helmi T, Cheraghian B. Oxygen tension in the aqueous humor of human eyes under different oxygenation conditions. *J Ophthalmic Vis Res*. 2013;8: 119–125.

40. Kwan M, Niinikoski J, Hunt TK. In vivo measurements of oxygen tension in the cornea, aqueous humor, and anterior lens of the open eye. *Invest Ophthalmol*. 1972;11:108–114.

41. Siegfried CJ, Shui Y-B, Holekamp NM, Bai F, Beebe DC. Oxygen distribution in the human eye: relevance to the etiology of open-angle glaucoma after vitrectomy. *Invest Ophthalmol Vis Sci*. 2010; 51:5731–5738.

42. Beebe DC, Shui Y-B, Siegfried CJ, Holekamp NM, Bai F. Preserve the (intraocular) environment: the importance of maintaining normal oxygen gradients in the eye. *Jpn J Ophthalmol*. 2014;58:225–231.

43. Leung BK, Bonanno JA, Radke CJ. Oxygen-deficient metabolism and corneal edema. *Prog Retin Eye Res*. 2011;30:471–492.

44. Mayordomo-Febrer A, Lopez-Murcia M, Morales-Tatay JM, Monleon-Salvado D, Pinazo-Duran MD. Metabolomics of the aqueous humor in the rat glaucoma model induced by a series of intracamerular sodium hyaluronate injection. *Exp Eye Res*. 2015;131:84–92.

45. Löbler M, Rehmer A, Guthoff R, Martin H, Sternberg K, Stachs O. Suitability and calibration of a rebound tonometer to measure IOP in rabbit and pig eyes. *Vet Ophthalmol*. 2011;14:66–68.